

A Method to Control Distributed Energy Resources in Distribution Networks Using Smart Meter Data

Yasin Zabihinia Gerdroodbari, Abu Bakr Pengwah, *Student Member, IEEE*, Reza Razzaghi, *Senior Member, IEEE*, Rahmat Heidari, and Lachlan L. H. Andrew, *Senior Member, IEEE*

Abstract—Voltage regulation has been one of the major challenges for distribution network operators (DNOs) due to the integration of distributed energy resources in the recent years. Control approaches mitigating over-voltage (OV) generally require full network model, which for low-voltage distribution networks (LVDNs), can be inaccessible to DNOs. This paper presents a novel data-driven model-free control framework for improving voltage regulation in 4-wire 3-phase LVDNs. In the proposed approach, first, using smart meter data, the aggregated resistance and reactance matrices of the network is estimated. Then, these matrices serve as an input for the proposed optimal power flow (OPF) method to control the DERs’ active and reactive power outputs. This method also lets the DNO adjust the fairness in prosumers’ generation curtailment. The performance of the proposed approach is evaluated in various case studies conducted on a real-world low-voltage test feeder. The simulation results exhibit significant effectiveness in solving the OV problem associated with DERs.

Index Terms—Over-voltage, voltage regulation, prosumers, data-driven OPF, smart meters.

I. INTRODUCTION

RECENTLY, the adoption of distributed energy resources (DERs), such as photovoltaic systems (PVs), has increased dramatically in many countries such as Australia [1]. Despite their environmental and economic benefits, DERs can result in several operational issues at the distribution level. Conventional distribution networks are designed for unidirectional power flow, from the upstream network to the customers. However, injection of power by DERs of customers (henceforth referred to as “prosumers”) can result in bidirectional power flows and undesired voltage rise, i.e., over-voltage (OV). To mitigate this problem, distribution network operators (DNOs) can employ various techniques, such as D-STATCOMs (e.g., [2]), distribution transformers with on-load tap changers (e.g., [3]), and grid reinforcement [4]. However, these solutions require additional investments and may have limited effectiveness in DER-rich networks.

A. Background and Literature Review

The *Volt-Watt* and *Volt-VAr* control in DERs can be considered as one of the most straightforward local voltage control solutions [5], [6]. In the *Volt-VAr* response mode, a DER adjusts its output reactive power according to the voltage measured at its point of connection. While in the *Volt-Watt* control, its output active power will be curtailed if the measured voltage is above a certain value. These approaches do not require any communication infrastructure and are

utilized as low-cost solutions. However, due to the utilization of local control input (i.e., terminal voltage), they may result in some undesired outcomes. Particularly, the *Volt-Watt* response mode can result in unequal active power curtailment of DERs across a feeder. This matter is aggravated in long feeders, as DERs far from the distribution transformers experience higher voltage rise and consequently, higher curtailment [7]. Moreover, due to the lack of coordination, DERs may not be optimally controlled in different demand scenarios and network conditions.

Coordinated control of DERs has been a topic of various research studies, and different control objectives have been considered. Studies such as [8], [9], focus on the management of voltage using DERs’ reactive power control capability. However, due to the high R/X ratio in distribution networks, the effectiveness of these methods may be limited. On the other hand, studies such as [10]–[12] consider the active power control of DER. However, solely relying on active power control can result in unnecessary curtailment imposed onto prosumers. Hence, in order to utilize the full capability of DERs, the methods presented in [13]–[15], allow the DNO to adjust both the active and reactive power outputs of DERs.

Incorporation of fairness in active power curtailment has also been pursued in recent studies. Various definitions of fairness have been proposed, in which prosumers curtail with respect to (i) their DERs planning generation power [10], [15], [16]; (ii) their planning export power [17], i.e., the DERs planning generation power minus their demand; (iii) their maximum generation in network’s minimum hosting capacity (NMHC) [18], i.e., the maximum generation of each prosumer when all demands are zero and DERs not providing reactive power compensation. Among these, the third definition considers prosumers’ local demand as well as network characteristic, in which as long as any prosumers’ planned export power is within the NMHC, they do not need to curtail. In addition, having an adjustable fairness is an important aspect specifically from the DNO’s point of view, since in general, there is a trade off between the total generation in a network and fairness in the generation curtailment. This has been discussed in [17] where the second definition (i.e., curtailing with respect to prosumers’ planning export power) of fairness has been used. In this work, fairness is adjusted by a coefficient in its objective function. However, the introduction of this heuristic coefficient comes with the downside of determining its optimal value (with respect to fairness) for different networks. In summary, the main drawback of the aforementioned coordinated control strategies is that they require the complete network model,

which may not be fully accessible in low-voltage distribution networks (LVDNs). Hence, data-driven approaches have been proposed to estimate the network model and its parameters from measurements.

The first class of approaches seeks to identify the network impedance model using measurements from additional metering devices. In [19], data obtained from line sensors is used while in [20], [21] measurements of voltage phase angles and current phase angles, obtained from phasor measurement units (PMUs), are processed to estimate the network impedance model. The cost and complexity of observing distribution networks using these extra measurement devices have motivated studies to identify the network model from the existing measurement infrastructure. The advent and extensive deployment of smart meters, used for billing and operational purposes, has opened up data-driven approaches that can estimate the network model from measurements sampled every few minutes.

Smart meter measurements have been employed in various applications, notably voltage control, state estimation, fault detection, among others. In the context of network model estimation, the authors in [22] present a regression technique based on the linearized equations of power flow that estimates the voltage sensitivity coefficients of a distribution network. Voltage sensitivity coefficients inherently describe the network model by relating the consumption data to the measured voltages and are widely used for various applications including DER control [23] and topology or network parameter estimation [24]–[26]. In [23], these coefficients are estimated through a regression process and are used to control PV inverters. Other means of estimating those coefficients include maximum likelihood approaches detailed in [24], [25] and the Newton Raphson based approach presented in [26], with all the aforementioned papers seeking to recover the distribution network topology. The main drawback of these papers is the negligence of the coupling between phases (including the neutral voltage) in 3-phase low-voltage distribution networks.

B. Contributions

In this paper, a novel framework to control the active and reactive power outputs of DERs that does not require the network model is proposed. This framework includes two parts for which their main contribution can be summarized as follows:

- An approach to estimate the network impedance model of 4-wire 3-phase LVDNs utilizing the smart-meter data, where the phases mutual coupling are represented by a resistance and reactance matrix;
- On-line control of the active and reactive power of DERs that incorporates an adjustable fairness objective with respect to the network's minimum hosting capacity;
- a data-driven control method that is robust against measurement noise.

C. Paper Organization

The rest of this paper is organized as follows; in Section II, the detail of the proposed optimal power flow (OPF) based on

the network impedance matrices is presented. The proposed method for estimating the network impedance matrices is presented in Section III. Section IV demonstrates the performance of the proposed approach on a real low-voltage test feeder. Finally, the concluding remarks are outlined in Section V.

II. ONLINE CONTROL OF DERS

This section describes the proposed 3-phase unbalanced OPF problem for the online control of DERs and the voltage management in the network. The proposed OPF formulation utilizes both active and reactive power control to minimize the curtailment. At the same time, it allows adjustable fairness in the curtailment of prosumers.

A. Objective Function

A common goal of the online control of DERs is to maximize the total harvested power of the DERs at each time step, t . However, this may cause unnecessary reactive power compensation by DERs. Thus, a small positive regularizing term $\lambda|Q|$ with $\lambda \ll 1$ is introduced, giving

$$\begin{aligned} \max_{P_{h,t}^{DER}, Q_{h,t}^{DER}} \sum_{h \in \mathcal{H}} P_{h,t}^{DER} - \lambda |Q_{h,t}^{DER}|, \\ \text{subject to. (8) – (13)}, \end{aligned} \quad (1)$$

where $P_{h,t}^{DER}$ and $Q_{h,t}^{DER}$ are the active and reactive power outputs of the installed DER at prosumer h , respectively. The rest of this section explains the approach to calculate the constraints of the optimization.

B. LVDN Formulation

The exported active and reactive powers of prosumers are

$$P_{h,t} = P_{h,t}^{DER} - P_{h,t}^{ld}, \quad (2)$$

$$Q_{h,t} = Q_{h,t}^{DER} - Q_{h,t}^{ld}, \quad (3)$$

where $P_{h,t}^{ld}$ and $Q_{h,t}^{ld}$ are the active and reactive power demand of prosumer h , respectively. The real and imaginary parts of prosumers' current are given by

$$I_{h,t}^{re} = \frac{P_{h,t} \cos(\tilde{\varphi}_{h,t})}{\tilde{V}_{h,t}} + \frac{Q_{h,t} \sin(\tilde{\varphi}_{h,t})}{\tilde{V}_{h,t}}, \quad (4)$$

$$I_{h,t}^{im} = -\frac{P_{h,t} \sin(\tilde{\varphi}_{h,t})}{\tilde{V}_{h,t}} + \frac{Q_{h,t} \cos(\tilde{\varphi}_{h,t})}{\tilde{V}_{h,t}}, \quad (5)$$

where $\tilde{V}_{h,t}$, and $\tilde{\varphi}_{h,t}$ are the predefined voltage magnitude (e.g., 1 pu), and predefined voltage phase angle, respectively. Using (4) and (5), the real and imaginary parts of each prosumer voltage can be calculated as

$$[V_{h,t}^{re}] = [V_t^{nl,re}] + [R][I_{h,t}^{re}] + [X][I_{h,t}^{im}], \quad (6)$$

$$[V_{h,t}^{im}] = [V_t^{nl,im}] + [R][I_{h,t}^{im}] - [X][I_{h,t}^{re}], \quad (7)$$

where $[R]$ and $[X]$ are the aggregated impedance matrices of the network. The approach to estimate them without requiring the network topology and lines' impedance value is explained in Section III. Furthermore, $[V_t^{nl,re}]$ and $[V_t^{nl,im}]$ are the real and imaginary parts of the no-load voltage of the distribution transformer's secondary, respectively.

C. Constraints

1) *Network Constraints*: The main focus of this paper is to prevent the OV problem due to power injection by DERs. Hence, the constraint for the voltage magnitude is

$$V_{h,t}^{re2} + V_{h,t}^{im2} \leq \bar{V}^2, \quad \forall h \in \mathcal{H}, \quad (8)$$

where \bar{V} is the statutory voltage limit.

2) *DER Constraints*: The active power output of the DER is always between 0 and the maximum available active power generation ($\bar{P}_{h,t}^{DER}$),

$$0 \leq P_{h,t}^{DER} \leq \bar{P}_{h,t}^{DER}. \quad (9)$$

Moreover, according to standards such as AS477.2 [5], to prevent excessive transmission losses, DERs should operate above a certain power factor. This constraint is formulated as

$$|Q_{h,t}^{DER}| \leq \tan(\cos^{-1}(PF^{\min})) P_{h,t}^{DER}, \quad (10)$$

where PF^{\min} is the defined minimum DERs' operating power factor by the DNO. Finally, the total power of a DER should be less than its rated power

$$\sqrt{P_{h,t}^{DER2} + Q_{h,t}^{DER2}} \leq S_h^{DER,Nom}, \quad (11)$$

where $S_h^{DER,Nom}$ is the rated power of prosumer h 's DER.

3) *Fairness Constraints*: There are multiple ways to improve fairness in power curtailment. Unfairness can be a penalty in the objective function [16], or a hard constraint can be imposed on unfairness. As described in the literature review, several definitions of fairness have been used in recent studies, where prosumers curtail fairly with respect to their maximum available generation, export power or NMHC. In this paper, similar to [18], a hard fairness constraint is considered. In this model, each prosumer h is allocated a threshold $P_{h,0}$ that determines the maximum allowed export power without requiring to curtail. This threshold can incorporate factors such as the location of the prosumer in the network and the capacity of the DER. The process of calculating $P_{h,0}$ is explained in Section II-D. If a prosumer's planned export power at time t is $\bar{P}_{h,t}^{DER} - P_{h,t}^{ld} < P_{h,0}$, then this is within the NMHC and no curtailment is needed, i.e.,

$$P_{h,t}^{DER} = \bar{P}_{h,t}^{DER}, \quad \forall h \in \mathcal{H}, \quad \text{with } \bar{P}_{h,t}^{DER} - P_{h,t}^{ld} \leq P_{h,0}, \quad (12)$$

otherwise the prosumer should curtail. To achieve fairness, a new index, FI , is introduced. For all prosumers $h, k \in \mathcal{H}$ connected to the same phase and with planned export power to the grid greater than $P_{h,0}$, it is required that

$$\left| \frac{\bar{P}_{h,t}^{DER} - P_{h,t}^{DER}}{\bar{P}_{h,t}^{DER} - P_{h,t}^{ld} - P_{h,0}} - \frac{\bar{P}_{k,t}^{DER} - P_{k,t}^{DER}}{\bar{P}_{k,t}^{DER} - P_{k,t}^{ld} - P_{k,0}} \right| \leq FI, \quad (13)$$

to ensure that the difference in prosumers' curtailment is always below the defined limit, DNOs can set the fairness index between $0 \leq FI \leq 1$. Lower values of FI result in more even power quality responses by prosumers, but possibly less efficient use of DERs.

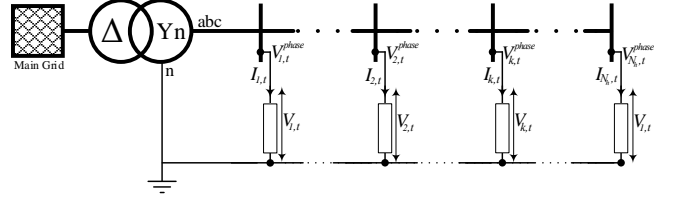


Fig. 1. A 4-wire 3-phase radial LVDN.

D. Calculation of $P_{h,0}$

In this section, the maximum generation of prosumers in the NMHC condition, $P_{h,0}$, is calculated. Note that $P_{h,0}$ is calculated once, provided that the network topology remains unchanged. The minimum hosting capacity of a network occurs when all loads are 0, i.e., $P_h^{ld} = 0$ and $Q_h^{ld} = 0$, and DERs' reactive power capability is disabled, i.e., $Q_h^{DER} = 0$. Therefore, the maximum generation of prosumers can be calculated where the objective function is

$$\max_{P_{h,0}} \sum_{h \in \mathcal{H}} P_{h,0}, \quad (14)$$

subject to (8) – (11) and (15).

In this case, the network formulation (Section II-B) and the constraints on the network (Section II-C1) and DERs (Section II-C2) are the same. However, since $P_{h,0}$ is not calculated, instead of applying (12) and (13), the constraint

$$\left| \frac{P_{h,0}}{S_h^{DER,Nom}} - \frac{P_{k,0}}{S_k^{DER,Nom}} \right| \leq FI, \quad (15)$$

is used.

III. NETWORK $[R]$ AND $[X]$ MATRICES ESTIMATION

With the full network model not readily accessible to DNOs, a method that estimates the network impedance model, which includes the resistance $[R]$ and reactance $[X]$ matrices, from smart meter measurements is proposed. These matrices are directly linked to the voltage sensitivity coefficients. First, a brief representation of a distribution network is provided, following which the voltage sensitivity coefficients are presented. Then, the proposed linear programming used to solve for the $[R]$ and $[X]$ matrices of the network is described. The formulation also includes linear constraints derived from the physical properties of distribution networks.

A. Background

In a typical 4-wire 3-phase radial low-voltage distribution network with $h \in \mathcal{H}$ prosumers (see Fig. 1), the voltage change of prosumer h at time t is given by

$$\begin{aligned} \Delta V_{h,t} &= \Delta V_{h,t}^{phase} + \Delta V_{h,t}^{mutual} = \\ &= \sum_{k \in \mathcal{H}} (R_{hk}^{phase} + jX_{hk}^{phase}) I_{k,t} + \sum_{k \in \mathcal{H}} (R_{hk}^{mutual} + jX_{hk}^{mutual}) I_{k,t}, \end{aligned} \quad (16)$$

where $\Delta V_{h,t}^{phase}$ is the voltage change caused by the prosumers connected to the same phase. Moreover, $\Delta V_{h,t}^{mutual}$

is the voltage change caused by all prosumers via coupling between phases (including the impact of neutral voltage). $I_{k,t}$ is the current of the k^{th} prosumer. R_{hk}^{phase} and X_{hk}^{phase} are the resistance and reactance of the common path between prosumers h and k to the distribution transformer if they are connected to the same phase, otherwise, both are 0. R_{hk}^{mutual} and X_{hk}^{mutual} are the mutual resistance and reactance between h and k , respectively [7]. Accordingly, (16) can be rewritten as

$$\Delta V_{h,t} = \sum_{k \in \mathcal{K}} (R_{hk} + jX_{hk}) I_{k,t}, \quad (17)$$

where $R_{hk} = R_{hk}^{phase} + R_{hk}^{mutual}$ and $X_{hk} = X_{hk}^{phase} + X_{hk}^{mutual}$. In another word, R_{hk} and X_{hk} are the aggregated impedance matrices of the network, which relate the voltage change of a prosumer to its own current and the others. The rest of this section is dedicated to the details of estimating R_{hk} and X_{hk} which will be used in the active and reactive power control of prosumers.

B. Voltage Sensitivity Coefficients

Voltage sensitivity coefficients relate the change in power consumption of prosumers to the change in the measured voltage levels. Traditionally, DNOs have been using voltage sensitivity coefficients in various applications including voltage control, planning, maintenance, and improving visibility of distribution networks [23]–[26]. It is not cost-efficient and practical for DNOs to install smart meters at all buses in the distribution network. As such, in this paper, reduced sensitivity matrices are considered where smart meter measurements obtained solely from prosumers (installed on the edges of the network) are processed. From [22], the voltage sensitivity matrices $[S^p]$ and $[S^q]$ can be expressed by

$$[\Delta V] = [S^p][P] + [S^q][Q], \quad (18)$$

where $[\Delta V]$, $[P]$ and $[Q]$ are the $N_h \times T$ matrices of voltage magnitude changes, active and reactive power exports, respectively. The total number of prosumers and sampled measurements are denoted by N_h and T , respectively. For 4-wire 3-phase systems, (18) is extended to

$$\begin{aligned} [\Delta V_a] &= [S_{aa}^p][P_a] + [S_{aa}^q][Q_a] + [S_{ab}^p][P_b] \\ &+ [S_{ab}^q][Q_b] + [S_{ac}^p][P_c] + [S_{ac}^q][Q_c], \end{aligned} \quad (19)$$

with the formulations for $[\Delta V_b]$ and $[\Delta V_c]$ defined analogously. The matrices $[P_\phi]$ and $[Q_\phi]$, where $\phi \in \{a, b, c\}$, are the active and reactive power exports of prosumers on phase ϕ . Following (17) and the $\mp 120^\circ$ degrees phase shift between the measurements on different phases, for any two prosumers h and k , the sensitivity coefficients can be expressed by

$$S_{hk}^p = \frac{1}{\tilde{V}} \sum_{k \in \mathcal{K}} \alpha_{\phi_h \phi_k}^p R_{hk} + \beta_{\phi_h \phi_k}^p X_{hk}, \quad \phi \in \{a, b, c\}, \quad (20)$$

$$S_{hk}^q = \frac{1}{\tilde{V}} \sum_{k \in \mathcal{K}} \alpha_{\phi_h \phi_k}^q R_{hk} + \beta_{\phi_h \phi_k}^q X_{hk}, \quad \phi \in \{a, b, c\}, \quad (21)$$

where \tilde{V} is 1 pu and the coefficients α and β depend on the phase connections of prosumers h and k . For instance, if

both prosumers are on similar phases, α^p and β^q are equal to one while β^p and α^q are zero. The expressions (20) and (21) also account for the impedance values, notably the neutral impedance, arising from the coupling of phase conductors of different feeders.

Following (20) and (21), (19) can be re-written with $[R]$ and $[X]$ being the decision variables. After deriving the coefficients α and β from [8], the $[R]$ and $[X]$ equations for all three phases A , B and C are

$$\begin{aligned} [\Delta V_a] &= [R_{aa}][P_a] + [X_{aa}][Q_a] + \\ [R_{ab}] &\left(-\frac{1}{2}[P_b] - \frac{\sqrt{3}}{2}[Q_b]\right) + [X_{ab}]\left(\frac{\sqrt{3}}{2}[P_b] - \frac{1}{2}[Q_b]\right) + \\ [R_{ac}] &\left(-\frac{1}{2}[P_c] + \frac{\sqrt{3}}{2}[Q_c]\right) + [X_{ac}]\left(-\frac{\sqrt{3}}{2}[P_c] - \frac{1}{2}[Q_c]\right), \end{aligned} \quad (22)$$

$$\begin{aligned} [\Delta V_b] &= [R_{bb}][P_b] + [X_{bb}][Q_b] + \\ [R_{ba}] &\left(-\frac{1}{2}[P_a] + \frac{\sqrt{3}}{2}[Q_a]\right) + [X_{ba}]\left(-\frac{\sqrt{3}}{2}[P_a] - \frac{1}{2}[Q_a]\right) \\ &+ [R_{bc}]\left(-\frac{1}{2}[P_c] - \frac{\sqrt{3}}{2}[Q_c]\right) + [X_{bc}]\left(\frac{\sqrt{3}}{2}[P_c] - \frac{1}{2}[Q_c]\right), \end{aligned} \quad (23)$$

$$\begin{aligned} [\Delta V_c] &= [R_{cc}][P_c] + [X_{cc}][Q_c] + \\ [R_{ca}] &\left(-\frac{1}{2}[P_a] - \frac{\sqrt{3}}{2}[Q_a]\right) + [X_{ca}]\left(\frac{\sqrt{3}}{2}[P_a] - \frac{1}{2}[Q_a]\right) + \\ [R_{cb}] &\left(-\frac{1}{2}[P_b] + \frac{\sqrt{3}}{2}[Q_b]\right) + [X_{cb}]\left(-\frac{\sqrt{3}}{2}[P_b] - \frac{1}{2}[Q_b]\right). \end{aligned} \quad (24)$$

The problem of phase identification using smart meter data has been extensively researched and is not the main focus of this paper. For this paper, the approach presented in [27] is implemented. The variations in voltage magnitudes of prosumers on similar phases is highly correlated. This feature is captured by a similarity matrix that measures the pairwise difference between voltage magnitudes of prosumers. The high dimensional data is reduced to a lower dimension using Singular Vector Decomposition (SVD) onto which K -means clustering is applied, returning three clusters for the 3 phases. The smart meter measurements are grouped according to the returned clusters.

The active and reactive power exports together with their respective coefficients can be pre-calculated from the smart meter measurements and the knowledge of the phases allocated to prosumers. Let $[\mathcal{P}_\phi]$ and $[\mathcal{Q}_\phi]$ represent the pre-calculated and vertically concatenated measurements to the horizontally concatenated $[R_\phi]$ and $[X_\phi]$ matrices, respectively (e.g., $[R_a] = [R_{aa} \ R_{ab} \ R_{ac}]$). This simplifies (22), (23) and (24) to

$$[\Delta V_a] = [R_a][\mathcal{P}_a] + [X_a][\mathcal{Q}_a], \quad (25)$$

$$[\Delta V_b] = [R_b][\mathcal{P}_b] + [X_b][\mathcal{Q}_b], \quad (26)$$

$$[\Delta V_c] = [R_c][\mathcal{P}_c] + [X_c][\mathcal{Q}_c], \quad (27)$$

respectively.

The overall objective of estimating $[R_\phi]$ and $[X_\phi]$ can be solved as a single linear problem. First, the measurement matrices (25),(26),(27) are diagonally concatenated into block diagonal matrices. With \oplus denoting block diagonal concatenation, if the voltages are given as

$$y = [\Delta V_a] \oplus [\Delta V_b] \oplus [\Delta V_c], \quad (28)$$

and pre-calculated active and reactive power exports as

$$A = \begin{bmatrix} \mathcal{P}_a \\ \mathcal{Q}_a \end{bmatrix} \oplus \begin{bmatrix} \mathcal{P}_b \\ \mathcal{Q}_b \end{bmatrix} \oplus \begin{bmatrix} \mathcal{P}_c \\ \mathcal{Q}_c \end{bmatrix}, \quad (29)$$

the $[R]$ and $[X]$ matrices can be solved for, in polynomial time, by minimizing the following least squares error function

$$\min_{R, X} \|y - [R \ X] A\|_2, \quad (30)$$

subject to. (31) – (32).

The $[R]$ and $[X]$ matrices are the reduced set of three phase sensitivity matrices and are each of size N_h by N_h . The constraints (31)-(32) imposed on the $[R]$ and $[X]$ matrices are described in the following section.

C. R and X Constraints

The constraints, imposed onto (30), are derived from the physical properties of the network [25]. As written in (17), the estimated R_{hk} and X_{hk} correspond to the impedance found in the common path linking the two prosumers, h and k , to the distribution transformer. With the distribution network being radial, for prosumers found on similar phase ϕ , the common path between the prosumers h and k to the transformer is similar to the common path between the prosumers k and h to the transformer. This leads to the symmetric constraint

$$R_{hk} = R_{kh}, \quad X_{hk} = X_{kh}, \quad (31)$$

which is also convex. The symmetric constraint cannot be imposed for prosumers located on different phases due to the asymmetry in the geometry of the three phase wires.

Finally, the impedance found in the common path between any two prosumers h and k (off-diagonal elements), must be less than or equal to the self impedance of the prosumers h and k (main diagonal elements). This translates to

$$R_{hk} \leq R_{hh}, \quad X_{hk} \leq X_{hh}. \quad (32)$$

IV. PERFORMANCE EVALUATION

In this section, the performance of the proposed framework has been evaluated on six simulation studies: (i) effectiveness in a PV-rich residential real-scale LVDN; (ii) Sensitivity analysis on the impact of errors in smart meter measurements; (iii) Impact of the fairness index on the active power curtailment of the prosumers; (iv) Impact of utilizing DERs' reactive power control capability on their active power curtailment; (v) analysis of the computation time for the $[R]$ and $[X]$ estimation process.

To this end, the 3-phase 4-wire network shown in Fig. 2 has been used. This network is adopted from 'ENWL' networks [28] (Network 5, Feeder 1) and scaled up to include an explicit neutral with the impedance data developed by Urquhart and

Thomson [29] and investigated as part of a larger study in [30]. It consists of 49 prosumers among which 17 are connected to phase A, 17 to phase B and 15 to phase C. These prosumers are equipped with PVs with the capacities of 4, 6, and 8 kW, as shown in Fig. 2. Moreover, the adopted solar irradiance profile is for a clear-sky day in Melbourne, Australia, to consider the worst-case scenario in terms of voltage management. The rest of specifications of this network such as prosumers demand data and network parameters are provided in [28] and are not reported here. For the simulation studies, the control framework has been implemented in Python, and Mosek has been utilized to solve the optimization problems. The time series (Quasi-Dynamic) 3-phase 4-wire power flow analysis is performed using OpenDSS. In these studies, $\lambda = 1e^{-6}$ and the limit for the OV is considered as 1.1 pu, based on AS4777.1 [31]. Furthermore, $FI = 0.25$ for all studies except Section IV-C.

A. PV-Rich Residential LVDN

1) *Voltage management using accurate network model:* Let us first consider the situation in which PVs are not controlled. Fig. 3 shows that the maximum voltage magnitude across all three phases exceeds the permissible limit of 1.1 pu. Although, since phase C has less installed PVS capacity than the other two phases, prosumers on this phase experience moderate OV. Then, the DERs are controlled using the proposed control approach presented in Section II, where the input $[R]$ and $[X]$ matrices are derived from the accurate network data. The result is shown in Fig. 4 (blue box plots), in which OV is fully resolved, and in all three phases the maximum voltage is limited to 1.1 pu.

2) *Voltage management using estimated network model:* In order to estimate the $[R]$ and $[X]$ matrices of the network, the sampled measurements of V , P , and Q by smart meters are utilized. In these measurements, the recording interval is 5 minutes, and approximately a month's worth of sampled data is used. Using this number of measurements leads to an over-determined system of linear equations ($T > 2N_h$) that can be approximately solved using the proposed minimization approach in Section III. Before solving (30), first, the phase classification of prosumers is identified using the phase identification algorithm in [27].

The optimization problem in 30 is formulated and solved using MOSEK. The resulting $[R]$ and $[X]$ matrices are then given as inputs to the DERs control algorithm. The impact of using the estimated $[R]$ and $[X]$ matrices can be seen in Fig. 4 (red box plots), where the voltage management performance does not change significantly. The maximum voltage in each phase is capped to 1.1 pu, similar to using the actual network model. In Fig. 5 and 6 the element-wise error of $[R]$ and $[X]$ are shown. In both of them, when prosumers are connected to the same phase, the error between the actual values and the estimated ones is much less compared to cases where their phase connection is different. The maximum percentage errors for prosumers on the same phase are 0.54% and 1.08% for $[R]$ and $[X]$, respectively, in contrast to 0.93% and 2.97% for prosumers on different phases. This is due to the fact that in the

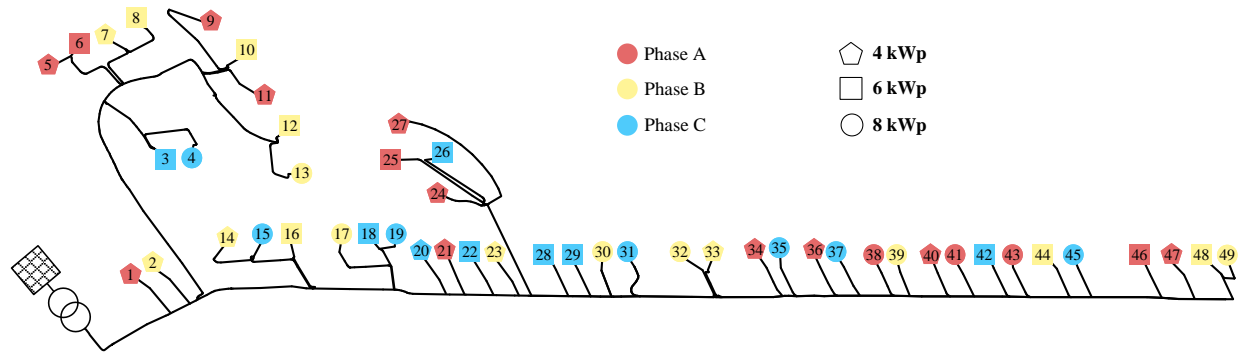


Fig. 2. Studied low-voltage test feeder; red, yellow, and blue prosumers are connected to phase A, B, and C, respectively.

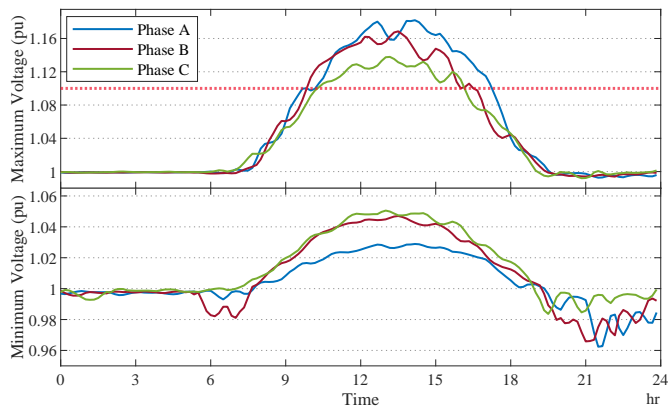


Fig. 3. Minimum and maximum voltage of the prosumers in each phase without any voltage management approach.

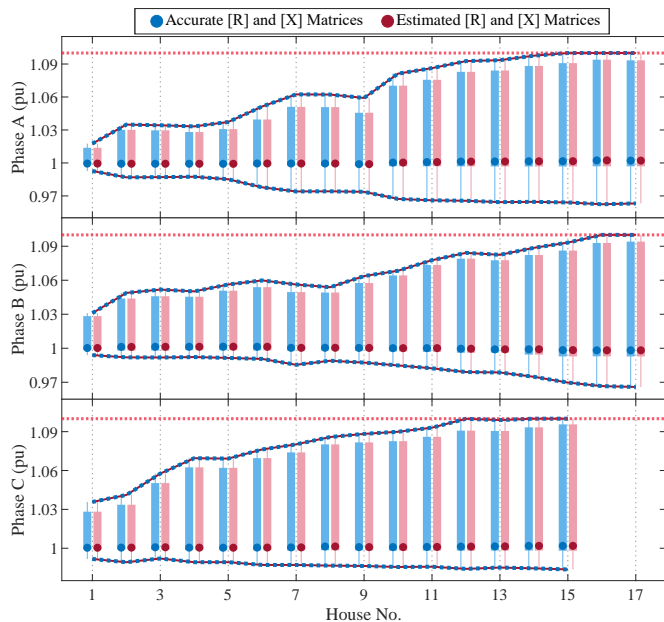


Fig. 4. Voltage of the prosumers when they are controlled with accurate and estimated network model.

estimation process, the angle difference between the phases is considered exactly as 120 degrees. Nonetheless, as the impact of prosumers connected to other phases is small compared to

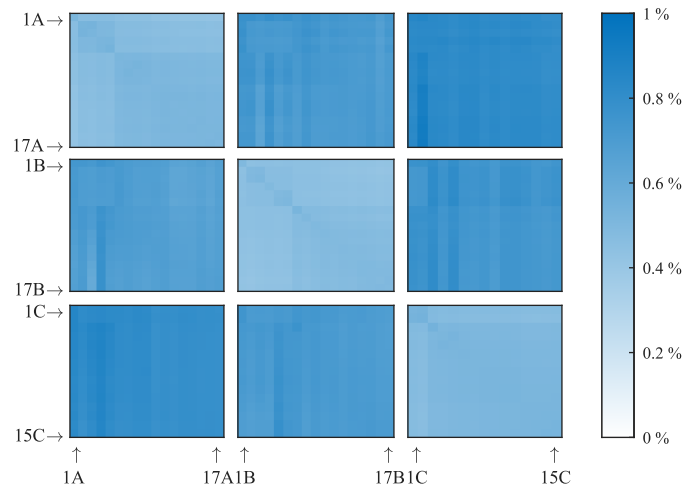


Fig. 5. Relative error in estimated $[R]$. Prosumers have been ordered according to their allocated phases.

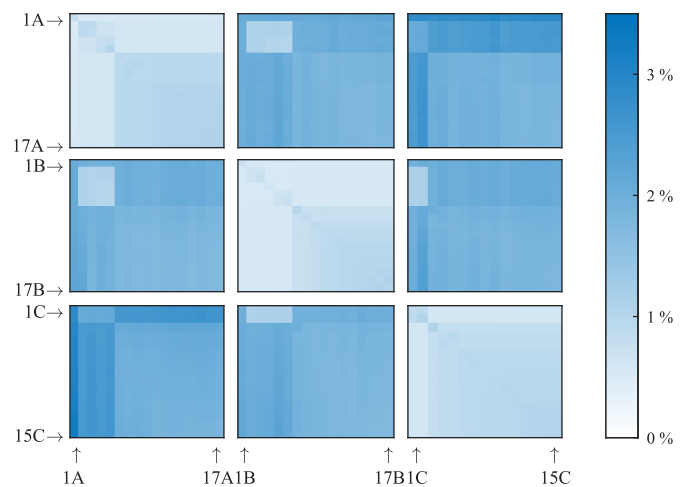


Fig. 6. Relative error in estimated $[X]$.

those connected to the same phase, this error does not result in a noticeable inaccuracy.

B. Impact of the Error in Measurements

The previous section evaluated the performance of the proposed method when the smart meter data had no measurement

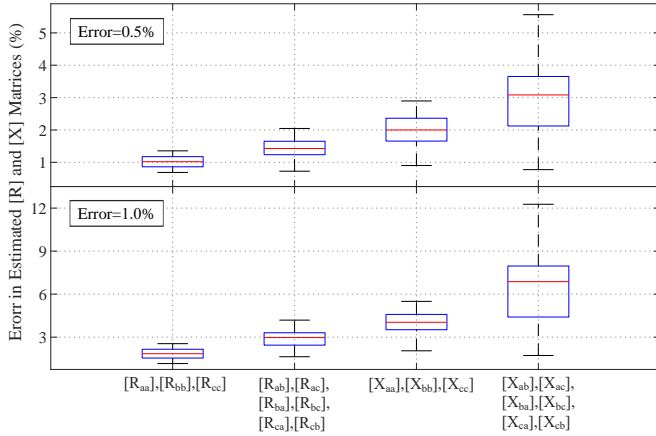


Fig. 7. Error of estimated $[R]$ and $[X]$ matrices when smart meter measurements have 0.5% (Top) and 1% (Bottom) error.

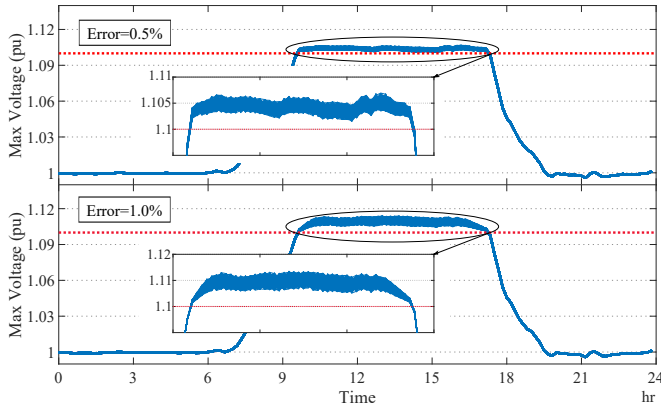


Fig. 8. Impact of 0.5% (Top) and 1% (Bottom) errors, in smart meter measurements, on the performance of the proposed approach in managing voltage.

errors. In this section, to assess the impact of measurement errors on the performance of the proposed framework, two error values, 0.5% and 1%, are added to the measurements of voltages, active and reactive powers [32] across the whole sampled period. The errors are sampled from independent truncated gaussian distributions with zero mean and standard deviation as one-third of the aforementioned maximum error values, in which values above the maximum error are truncated. In Fig. 7, the mismatch in the estimated $[R]$ and $[X]$ matrices for the errors of 0.5% and 1% are shown. Each box plot in this figure represents the variation in the maximum recorded error, for the particular sub-matrix, across all instances. The maximum error values for the main diagonals and the off-diagonal elements of $[R]$ and $[X]$ are separated into distinct boxplots since the impact of the main diagonal elements is more pronounced on the voltages. Similar to the previous study, the error in off-diagonal elements is more significant. This error has an impact on the voltage control method, as shown in Fig. 8. The error is higher during the high generation period when voltage management is required. However, the performance is not significantly impacted, and it is in an acceptable range.

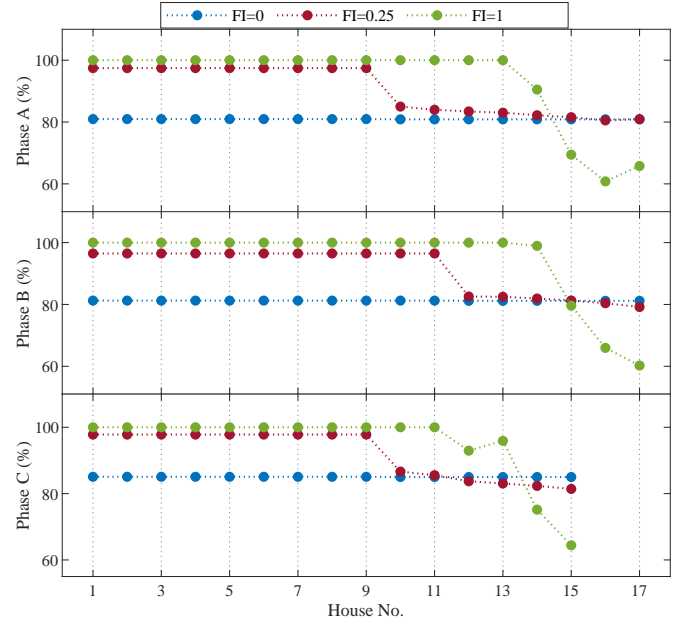


Fig. 9. The normalized prosumers export power with $FI = 0$, $FI = 0.25$, and $FI = 1$ (no limit).

C. Impact of the Fairness Index

The proposed framework allows DNOs to manage voltage with an adjustable fairness index using the control variable FI in (13). If $FI = 0$, DERs curtailment is equal and operation is completely fair according to this metric, while if $FI = 1$ (unlimited), the fairness is not a constraint. Generally, higher fairness, i.e., smaller FI , results in lower total generation in the grid [16], [17]. To study the impact of FI on the performance of the proposed method, three values of 0, 0.25, and 1 are considered. Fig. 9 shows the normalized total generated power by prosumers in these cases. Higher values of FI results in more uneven generation by prosumers. In particular, prosumers far from the distribution transformer experience higher curtailment. When there is no limit on FI , the total generation in the network increases to 1.749 MWh, while this is 1.672 and 1.613 MWh for $FI = 0.25$ and $FI = 0$.

D. Impact of the DERs Reactive Power Control Capability

The proposed voltage management approach utilizes both reactive and active power control. This leads to a reduction in the amount of active power that prosumers have to curtail and increases the energy available in the grid relative to the case where only the DERs' active power is controlled. To study this, two cases are considered: (i) DERs are equipped with reactive power control capability and (ii) DERs do not have this capability. In Fig. 10, the export active and reactive power of prosumer 48B is shown as an example. In both cases, this prosumer needs to curtail; however, reactive power compensation reduces the curtailed amount. This is shown by the green graph in which this prosumer exports 5.82% more, from 34.88 to 36.91 kWh in total for the day. From the network's point of view, prosumers collectively inject 5.66% more, 1.582 to 1.672 MWh using the reactive power support.

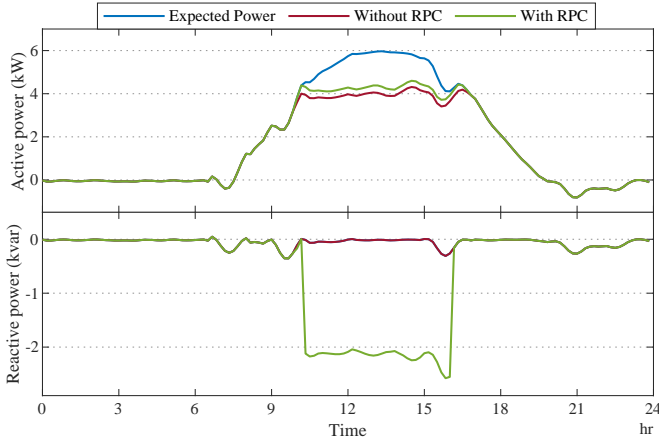


Fig. 10. The impact of reactive power control capability of prosumers.

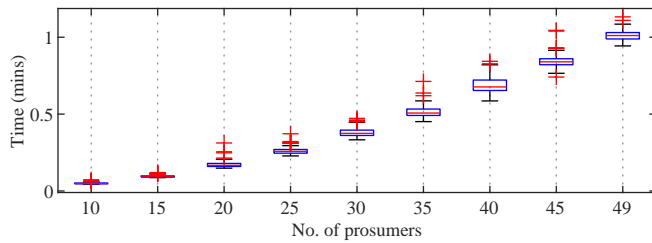


Fig. 11. Computation time of algorithm against various number of prosumers with t fixed to approximately 1 month.

E. Computational Complexity

While the DERs' voltage management is performed in real-time, the estimation of the $[R]$ and $[X]$ matrices is performed offline. The least squares formulation has computational complexity of $\mathcal{O}(N_h^3 + N_h^2 T)$ [33]. The number of prosumers has a significant contribution to the overall computation time. To study the impact of N_h , the network impedance estimation process (Section III) is applied on networks with various number of prosumers. The number of prosumers is varied from 10 to 49 in increments of 5, and the corresponding measurement matrices are given as input to the algorithm. A 6-core 3.2 GHz Intel Core i7 CPU with 32 GB memory is used for conducting the simulations. The processing time is recorded, and the experiment is repeated over multiple instances. The time cost of the algorithm is shown in Fig. 11. While there is an increase in the computation time going from $N_h = 10$ to $N_h = 49$ prosumers, it does not grow quadratically. The estimation of $[R]$ and $[X]$ matrices can be accomplished in near real-time with the worst time cost being 1 minute. If a cubic polynomial of the form $a_3 x^3 + a_2 x^2 + a_1 x + a_0$ is fitted to the mean computation times, the coefficient a_3 is 400 times smaller than a_2 while the latter is 6 times smaller than a_1 . This shows that exponents corresponding to polynomial degrees above 3 are not significant, and the growth in computation time will not drastically worsen as N_h increases.

V. CONCLUSION

This paper proposed a novel over-voltage mitigation algorithm. To this end, two new algorithms were devised. The first

estimates the distribution network impedance model in terms of the resistance and reactance matrices. The impedance model also includes the impedance due to the mutual coupling of phase conductors of different feeders. This is shown to produce more accurate estimates of resistance and reactance values. The second algorithm incorporates the estimated network impedance model into a quadratically constrained quadratic problem that solves for the optimum operating points of DERs, whilst accounting for fairness. The proposed OV mitigation algorithm has been shown to efficiently manage DER in a real LVDN, with the simulation case studies exhibiting the superior performance of the proposed algorithms.

REFERENCES

- [1] L. Wang, R. Yan, F. Bai, T. Saha, and K. Wang, "A distributed inter-phase coordination algorithm for voltage control with unbalanced pv integration in lv systems," *IEEE Trans. on Sustainable Energy*, vol. 11, no. 4, pp. 2687–2697, 2020.
- [2] C.-S. Chen, C.-H. Lin, W.-L. Hsieh, C.-T. Hsu, and T.-T. Ku, "Enhancement of pv penetration with dstacom in taipower distribution system," *IEEE Trans. on Power Systems*, vol. 28, no. 2, pp. 1560–1567, 2012.
- [3] S. Hashemi, J. Østergaard, T. Degner, R. Brandl, and W. Heckmann, "Efficient control of active transformers for increasing the pv hosting capacity of lv grids," *IEEE Trans. on Industrial Informatics*, vol. 13, no. 1, pp. 270–277, 2016.
- [4] M. Zeraati, M. E. H. Golshan, and J. M. Guerrero, "Voltage quality improvement in low voltage distribution networks using reactive power capability of single-phase pv inverters," *IEEE Transactions on Smart Grid*, vol. 10, no. 5, pp. 5057–5065, 2019.
- [5] AS/NZS Standard 4777.2:2015, *Grid Connection of Energy Systems via Inverters-Part 2: Inverter Requirements*, Oct. 2015.
- [6] European Standard NEN-EN 50438, *Requirements for Micro-Generating Plants to be Connected in Parallel With Public Low-Voltage Distribution Networks*, Dec. 2013.
- [7] Y. Z. Gerdroodbari, R. Razzaghi, and F. Shahnia, "Decentralized control strategy to improve fairness in active power curtailment of pv inverters in low-voltage distribution networks," *IEEE Transactions on Sustainable Energy*, vol. 12, no. 4, pp. 2282–2292, 2021.
- [8] —, "Improving voltage regulation and unbalance in distribution networks using peer-to-peer data sharing between single-phase pv inverters," *IEEE Transactions on Power Delivery*, vol. 37, no. 4, pp. 2629–2639, 2022.
- [9] A. Raghmi, G. Ledwich, and Y. Mishra, "Improved reactive power sharing among customers' inverters using online thevenin estimates," *IEEE Transactions on Power Systems*, vol. 34, no. 6, pp. 4168–4176, 2019.
- [10] S. Alyami, Y. Wang, C. Wang, J. Zhao, and B. Zhao, "Adaptive real power capping method for fair overvoltage regulation of distribution networks with high penetration of pv systems," *IEEE Trans. on Smart Grid*, vol. 5, no. 6, pp. 2729–2738, 2014.
- [11] Y. Wang, K. T. Tan, X. Y. Peng, and P. L. So, "Coordinated control of distributed energy-storage systems for voltage regulation in distribution networks," *IEEE Trans. on Power Delivery*, vol. 31, no. 3, pp. 1132–1141, 2016.
- [12] Y. Riffonneau, S. Bacha, F. Barruel, and S. Ploix, "Optimal power flow management for grid connected pv systems with batteries," *IEEE Trans. on Sustainable Energy*, vol. 2, no. 3, pp. 309–320, 2011.
- [13] B. Zhang, A. Y. Lam, A. D. Domínguez-García, and D. Tse, "An optimal and distributed method for voltage regulation in power distribution systems," *IEEE Transactions on Power Systems*, vol. 30, no. 4, pp. 1714–1726, 2015.
- [14] D. Gebbran, S. Mhanna, Y. Ma, A. C. Chapman, and G. Verbić, "Fair coordination of distributed energy resources with volt-var control and pv curtailment," *Applied Energy*, vol. 286, p. 116546, 2021.
- [15] F. Olivier, P. Aristidou, D. Ernst, and T. Van Cutsem, "Active management of low-voltage networks for mitigating overvoltages due to photovoltaic units," *IEEE Trans. on Smart Grid*, vol. 7, no. 2, pp. 926–936, 2016.
- [16] P. Lusis, L. L. H. Andrew, S. Chakraborty, A. Liebman, and G. Tack, "Reducing the unfairness of coordinated inverter dispatch in pv-rich distribution networks," in *2019 IEEE Milan PowerTech*, 2019, pp. 1–6.

- [17] P. Lusi, L. L. H. Andrew, A. Liebman, and G. Tack, "The added value of coordinating inverter control," *IEEE Transactions on Smart Grid*, vol. 12, no. 2, pp. 1238–1248, 2021.
- [18] Y. Zabihinia Gerdoodbari, M. Khorasany, and R. Razzaghi, "Dynamic pq operating envelopes for prosumers in distribution networks," *Applied Energy*, vol. 325, p. 119757, 2022.
- [19] M. Farajollahi, A. Shahsavari, and H. Mohsenian-Rad, "Topology identification in distribution systems using line current sensors: An MILP approach," *IEEE Trans. Smart Grid*, vol. 11, no. 2, pp. 1159–1170, 2019.
- [20] K. Moffat, M. Bariya, and A. Von Meier, "Unsupervised impedance and topology estimation of distribution networks—limitations and tools," *IEEE Trans. Smart Grid*, vol. 11, no. 1, pp. 846–856, 2019.
- [21] V. L. Srinivas and J. Wu, "Topology and parameter identification of distribution network using smart meter and μ pmu measurements," *IEEE Transactions on Instrumentation and Measurement*, vol. 71, pp. 1–14, 2022.
- [22] K. Christakou, J.-Y. LeBoudec, M. Paolone, and D.-C. Tomozei, "Efficient computation of sensitivity coefficients of node voltages and line currents in unbalanced radial electrical distribution networks," *IEEE Transactions on Smart Grid*, vol. 4, no. 2, pp. 741–750, 2013.
- [23] E. L. da Silva, A. M. N. Lima, M. B. de Rossiter Corrêa, M. A. Vitorino, and L. T. Barbosa, "Data-driven sensitivity coefficients estimation for cooperative control of pv inverters," *IEEE Transactions on Power Delivery*, vol. 35, no. 1, pp. 278–287, 2020.
- [24] V. C. Cunha, W. Freitas, F. C. L. Trindade, and S. Santoso, "Automated determination of topology and line parameters in low voltage systems using smart meters measurements," *IEEE Transactions on Smart Grid*, vol. 11, no. 6, pp. 5028–5038, 2020.
- [25] A. B. Pengwah, L. Fang, R. Razzaghi, and L. L. H. Andrew, "Topology identification of radial distribution networks using smart meter data," *IEEE Systems Journal*, pp. 1–12, 2021.
- [26] J. Zhang, Y. Wang, Y. Weng, and N. Zhang, "Topology identification and line parameter estimation for non-pmu distribution network: A numerical method," *IEEE Transactions on Smart Grid*, vol. 11, no. 5, pp. 4440–4453, 2020.
- [27] S. Liu, X. Cui, Z. Lin, Z. Lian, Z. Lin, F. Wen, Y. Ding, Q. Wang, L. Yang, R. Jin, and H. Qiu, "Practical method for mitigating three-phase unbalance based on data-driven user phase identification," *IEEE Transactions on Power Systems*, vol. 35, no. 2, pp. 1653–1656, 2020.
- [28] "Low voltage network solutions closedown report," Low Carbon Networks Fund, Tech. Rep. June, 2014.
- [29] A. J. Urquhart and M. Thomson, "Series impedance of distribution cables with sector-shaped conductors," *IET Gener. Transm. Distrib.*, vol. 9, no. 16, pp. 2679–2685, 2015.
- [30] F. Geth, R. Heidari, and A. Koirala, "Computational analysis of impedance transformations for four-wire power networks with sparse neutral grounding," in *ACM e-Energy (accepted)*, 2022, pp. 1–9.
- [31] AS/NZS Standard 4777.1:2016, *Grid Connection of Energy Systems via Inverters-Part 1: Installation Requirements*, Sep. 2016.
- [32] A. P. Grilo, P. Gao, W. Xu, and M. C. de Almeida, "Load monitoring using distributed voltage sensors and current estimation algorithms," *IEEE Transactions on Smart Grid*, vol. 5, no. 4, pp. 1920–1928, 2014.
- [33] L. El Ghaoui and H. Lebret, "Robust solutions to least-squares problems with uncertain data," *SIAM J. matrix analysis and applications*, vol. 18, no. 4, pp. 1035–1064, 1997.